Bachelor of Science (Research)
Material Science

INSPIRE Summer Project Report

The influence of Convection on the Evolution of Microstructure during Solidification

Submitted By:-
Apaar Shanker
(SR No. 09101)

Under the guidance of
Dr. Abhik Choudhury

Contents

Synopsis

Solidification is one of the major processing routes among the various materials processing techniques, where in there is phase transformation from a liquid to one or more solid-phases. The process gives rise to a variety of microstructures, arising out of dendritic, eutectic, peritectic and monotectic reactions. It is well known that properties of a material can be linked to its structure at the microscopic scale. Thus, in order to manufacture a cast product with desired properties, it is essential to determine the influence of the processing parameters on microstructural evolution. Here, modelling of complex microstructural evolution allows for the determination of the useful process $\rightarrow$ structure and parameter $\rightarrow$ structure correlations.

Being a first order phase transition, the solidification reaction involves a transfer of heat/mass across the interface between the solid and the liquid phases concomitant with diffusion in the bulk liquid and the solid phases. Any modelling technique describing this phenomenon will require, that in addition to the global boundary conditions controlling the heat/mass exchange, it self-consistently is able to integrate the transport processes at the moving interface between the evolving phases with those in the bulk.

Classically, such problems were treated with *Sharp-interface* methods, wherein, separate transport equations are solved in the respective bulk phases, while the appropriate (*Stefan-boundary*) conditions are imposed at the interface nodes which therefore need to be marked after each time iteration. The method becomes cumbersome in case of complex morphological evolution which is commonly encountered in most solidification reactions, where explicit interface tracking becomes computationally expensive and resolving sharp curvatures necessitates the use of finer meshes.

In this context, we resort to the *phase field method* - a state-of-the art technique, developed in the past three decades which obviates the need for tracking of the moving interfaces. Succinctly, the method describes evolution equations for order parameters varying smoothly between the various phases, thereby representing phase evolution. The various boundary conditions at the moving interface are self-consistently described in the transport equations describing solutal/heat/momentum transport, which are defined globally. The transport equations are coupled with the evolution equations for the order parameter. This class of methods has been applied to a variety of phase transformation reactions.

Presently, we have used the phase field method to investigate the influence of

convection on dendritic growth. There is a large practical interest in dendritic solidification as an overwhelming majority of metallic systems solidify in this manner. This is also an interesting problem in terms of mechanisms of pattern selection in a non-equilibrium systems and engenders a lot of theoretical interest.

The fundamental problem being addressed here is the selection of the scaling and growth velocities of the dendrites during solidification. The problem is well understood in the purely diffusive regime. However, in practical set-ups the dendrite growth is unavoidably influenced by buoyancy driven flows due to gravity. The effect is due to large scale transport of mass or heat by the fluid currents. This effect of fluid flow on the dendrite tip selection, however, has not yet been fully understand and is of great practical import.

In the present study we have endeavoured to throw some light this aspect of solidification. We have set up a phase field model based on the fundamental equations for solidification while incorporating flow in the fluid phase. We thus seek to directly simulate dendritic growth in a convective regime and gauge the effect of flow on the evolving morphology.

An introduction to Dendritic Solidification

Dendritic solidification is ubiquitous in material science and is of great practical and theoretical importance. The dendritic morphology can be characterised by growth of primary arms along well defined crystallographic directions with each primary arm also giving rise to self-similar secondary and tertiary arms. This self-similarity between the patterns at various length scales is a key characteristic of fractals and is observed commonly in nature. Dendritic micorstructures result as a destabilisation of a planar or spherical growth front. A critical component giving rise to dendritic growth, where the primary growth occurs along well defined growth directions, is the surface energy anisotropy.

Physically, an understanding of dendrite morphology and growth would entail the knowledge of the scaling laws pertaining to - dendrite tip radius, inter dendritic and secondary arm spacings and how they change as a function of the processing conditions, alloy composition and properties. The requirement for understanding the scale and variation of these parameters lies in the fact that macroscopic parameters such as tensile strength, fracture toughness etc. are often determined by the scale of the microstructure.

There have been significant advances in understanding the physics of dendrite growth. The role of crystalline anisotropy in the selection of the dendrite tip radius and velocity is well explained by the microsolvability theory [1]. The theory has been validated by sophisticated microgravity experiments as well as phase field simulations in both two and three dimensions, that focussed on the purely diffusive regime.

On earth, however, dedritic growth is almost unavoidably influenced by buoyancy driven mass and energy advection in the melt phase. Melt flow introduces a new length scale in the problem, viz. the length of the convecting rolls, and breaks the symmetry of transport depending on the direction of the vector of gravity relative to the direction of growth. Self-Organising pattern formation in solidification begins to compete with the self-organisation of the convection patterns. On the one hand, convective transport of solute significantly alters the growth conditions. On the other hand, the magnitude of convection critically depends on solute gradients due to growth and on the friction of the convecting liquid melt against the growing solid-liquid interface[3].

The Equations

3.1 The phasefield equations

We have derived the evolution equation of the phasefield variable to be,

$$\frac{\partial \phi}{\partial t} = -M\left(\frac{\partial f_o}{\partial \phi} - 2\kappa\nabla^2\phi\right) - M\underbrace{\left(c_l^{eq} - c_s^{eq}\right)\left(\mu - \mu_{eq}\right)\frac{\partial h\left(\phi\right)}{\partial \phi}}_{driving force}. \tag{3.1}$$

which is coupled with the evolution equation for diffusion potential μ as

$$\left(\frac{\partial c_s}{\partial \mu}h\left(\phi\right) + \frac{\partial c_l}{\partial \mu}(1 - h\left(\phi\right))\right)\frac{\partial \mu}{\partial t} = \nabla\cdot\left(M\nabla\mu\right) - \left(c_s\left(\mu\right) - c_l\left(\mu\right)\right)\frac{\partial h\left(\phi\right)}{\partial t} - \vec{v}\cdot\nabla c \tag{3.2}$$

For the sake of simplicity, in the present model we choose the following relations of c^s and c^l,

$$c^l\left(\mu\right) = \mu \tag{3.3}$$

$$c^s\left(\mu\right) = kc^l = k\mu \tag{3.4}$$

where k is the partition coefficient.

Then, the expression for driving force becomes

$$\Psi_l - \Psi_s = \left(c_s^{eq} - c_l^{eq}\right)\left(\mu - \mu_{eq}\right) \Rightarrow \Psi_l - \Psi_s = (k-1)\mu\left(\mu - \mu_{eq}\right) \tag{3.5}$$

The evolution equation for ϕ,, thus suitably modified, can be written as,

$$\frac{\partial \phi}{\partial t} = -M\left(\frac{\partial f_o}{\partial \phi} - 2\kappa\nabla^2\phi\right) - M\underbrace{(k-1)\mu\left(\mu - \mu_{eq}\right)\frac{\partial h\left(\phi\right)}{\partial \phi}}_{driving force}. \tag{3.6}$$

Also, we can consider χ such that,

$$\chi = \left(\frac{\partial c^s}{\partial \mu}h\left(\phi\right) + \frac{\partial c^l}{\partial \mu}(1 - h\left(\phi\right))\right) \tag{3.7}$$

$$\Rightarrow \chi = 1 + (k-1)\,h\left(\phi\right) \tag{3.8}$$

Then, the evolution equation for μ becomes,

$$\chi\left(\frac{\partial\mu}{\partial t}\right) = \nabla\cdot\left(M\nabla\mu\right) - \left(c^s\left(\mu\right) - c^l\left(\mu\right)\right)\frac{\partial h\left(\phi\right)}{\partial t} - \vec{v}\cdot\nabla c \tag{3.9}$$

$$\chi\left(\frac{\partial\mu}{\partial t}\right) = \nabla\cdot\left(M\nabla\mu\right) - \left(k-1\right)\mu\frac{\partial h\left(\phi\right)}{\partial t} - \vec{v}\cdot\nabla c \tag{3.10}$$

For the sake of reiteration, $\phi = 1 \Longrightarrow$ solid and $\phi = 0 \Longrightarrow$ liquid
Also, we have chosen the interpolation function $h(\phi)$ such that,

$$h(\phi) = \phi^2\left(3-2\phi\right) \tag{3.11}$$

$$\frac{\partial h(\phi)}{\partial\phi} = 6\phi\left(1-\phi\right) \tag{3.12}$$

We chose f_o to be the classic double well potential, given as,

$$f_o = 9\phi^2\left(1-\phi\right)^2 \tag{3.13}$$

We also factor in some constants in order to non-denationalise the equations: τ as relaxation time and ϵ as relaxation length and γ which corresponds to surface energy. Incorporating all this, the equation for evolution of the phase field variables can finally be written down as,

$$\tau\epsilon\frac{\partial\phi}{\partial t} = \gamma\nabla^2\phi - \frac{\gamma}{\epsilon}18\phi(1-\phi)(1-2\phi) + (k-1)\mu\left(\mu-\mu_{eq}\right)\left(6\phi\right)\left(1-\phi\right) \tag{3.14}$$

$$\chi\frac{\partial\mu}{\partial t} = M\nabla^2\mu - 6\left(k-1\right)\mu\phi\left(1-\phi\right)\frac{\partial\phi}{\partial t} - \vec{v}\cdot\nabla c \tag{3.15}$$

3.2 Incorporating Anisotropy

Our free energy functional is of the form,

$\mathcal{F} = \int_{-\infty}^{\infty}(\gamma\epsilon|\nabla\phi|^2 + \frac{\gamma}{\epsilon}9\phi^2(1-\phi)^2 + ...)dx$

We define an inter facial energy term with a small cubic anisotropy to the order of a few percent.

$a_c = \gamma_o\left(1-\delta_{\alpha\beta}cos(4\theta)\right)$
where $\delta_{\alpha\beta}$ is the strength of anisotropy.

Accordingly, the functional gets modified to be,
$\mathcal{F} = \int_{-\infty}^{\infty}(\gamma a_c^2(\theta)|\nabla\phi|^2 + \frac{\gamma}{\epsilon}9\phi^2(1-\phi)^2 + ...)dx$

The interface energy needs to be a function of interface normal. For this, we determine the following relation between interface normal $\vec{n}$ and θ which is the angle of orientation.

$\theta = tan^{-1}\left(\frac{n_x}{n_y}\right), cos\theta = n_x, sin\theta = n_y,\ \hat{n} = n_x\hat{i} + n_y\hat{j}$

$n_x^2 + n_y^2 = 1$

$$\hat{n} = \frac{\nabla\phi}{|\nabla\phi|}, n_x = \frac{\left(\frac{\partial\phi}{\partial x}\right)}{|\nabla\phi|}, n_y = \frac{\left(\frac{\partial\phi}{\partial y}\right)}{|\nabla\phi|}$$

We need to able to fully describe the anisotropy in terms of gradients in the ϕ field. To achieve this we resorted to the following treatment,

Expand $cos4\theta$ as,
$cos4\theta + isin4\theta = (cos\theta + isin\theta)^2$
on collecting the real terms we get
$cos4\theta = cos^4\theta + sin^4\theta - {}^4C_2 cos^2\theta sin^2\theta$
$= n_x^4 + n_y^4 - 6n_x^2 n_y^2$

using: $n_x^2 + n_y^2 = 1$
$\Rightarrow cos4\theta = 4(n_x^4 + n_y^4) - 3$
Now, $a_c = \gamma_o \left(1 - \delta_{\alpha\beta}\left(4\left(n_x^4 + n_y^4\right) - 3\right)\right)$

$$a_c = \gamma_o \left(1 - \delta_{\alpha\beta}\left(4\left(\frac{\frac{\partial\phi}{\partial x}^4 + \frac{\partial\phi}{\partial y}^4}{|\nabla\phi|^4}\right) - 3\right)\right)$$

call $\frac{\partial\phi}{\partial x} \rightarrow \phi_x$ and $\frac{\partial\phi}{\partial y} \rightarrow \phi_y$

$$a_c = \gamma_o \left(1 - \delta_{\alpha\beta}\left(4\left(\frac{\phi_x^4 + \phi_y^4}{\left(\phi_x^2 + \phi_y^2\right)^2}\right) - 3\right)\right)$$

The variational derivative operator expands as,

$$\frac{\delta}{\delta\phi} = \left(\frac{\partial}{\partial\phi} - \nabla\phi \cdot \frac{\partial}{\partial\nabla\phi}\right)$$

Then on incorporating anisotropy, the gradient energy term in the evolution equation gets modified as,

$$\frac{\delta}{\delta\phi}\left(a_c^2|\nabla\phi|^2\right) = \frac{\partial}{\partial\phi}\left(a_c^2|\nabla\phi|^2\right) - \nabla\phi \cdot \frac{\partial}{\partial\nabla\phi}\left(a_c^2|\nabla\phi|^2\right)$$

As both a_c and $|\nabla\phi|$ are a function of ϕ_x and ϕ_y only, the $\frac{\partial}{\partial\phi}$ term goes to zero.

Also, in Cartesian coordinates $\frac{\partial}{\partial\nabla\phi}$ can be written as,

$$\frac{\partial}{\partial\phi_x}\hat{i} + \frac{\partial}{\partial\phi_y}\hat{j}$$

As such, on including anisotropy the time evolution equation for the phase field variable becomes:

$$\tau\epsilon\frac{\partial\phi}{\partial t} = \gamma\epsilon\nabla\cdot\begin{pmatrix}\dfrac{\partial}{\partial\phi_x}\left(a_c|\nabla\phi|\right)^2\\ \dfrac{\partial}{\partial\phi_y}\left(a_c|\nabla\phi|\right)^2\end{pmatrix} - \frac{\gamma}{\epsilon}18\phi(1-\phi)(1-2\phi) + (k-1)\mu\left(\mu-\mu_{eq}\right)6\phi\left(1-\phi\right) \tag{3.16}$$

The individual components of the vector $\begin{pmatrix}\dfrac{\partial}{\partial\phi_x}\left(a_c|\nabla\phi|\right)^2\\ \dfrac{\partial}{\partial\phi_y}\left(a_c|\nabla\phi|\right)^2\end{pmatrix}$ when fully expanded look as follows,

$$\frac{\partial}{\partial\phi_x}\left(a_c|\nabla\phi|\right)^2 = 2a_c\phi_x\left(\gamma_o - \frac{16\gamma_o\delta\left(\phi_x^2\phi_y^2-\phi_y^4\right)+4\gamma_o\delta\left(\phi_x^4+\phi_y^4\right)}{\left(\phi_x^2+\phi_y^2\right)^2}+3\delta\right) \tag{3.17}$$

$$\frac{\partial}{\partial\phi_y}\left(a_c|\nabla\phi|\right)^2 = 2a_c\phi_y\left(\gamma_o - \frac{16\gamma_o\delta\left(\phi_y^2\phi_x^2-\phi_x^4\right)+4\gamma_o\delta\left(\phi_y^4+\phi_x 4\right)}{\left(\phi_y^2+\phi_x^2\right)^2}+3\delta\right) \tag{3.18}$$

where, $a_c = \gamma_o\left(1-\delta\left(4\left(\frac{\phi_x^4+\phi_y^4}{\left(\phi_x^2+\phi_y^2\right)^2}\right)\right)\right)$

3.3 Fluid Flow

The evolution equation for μ, derived from mass conservation, includes advection i.e. that is long range mass transport due to fluid currents.

$$\chi\frac{\partial\mu}{\partial t} = M\nabla^2\mu - 6\left(k-1\right)\mu\phi\left(1-\phi\right)\frac{\partial\phi}{\partial t} - \vec{v}\cdot\nabla c \tag{3.19}$$

The time evolution of velocity field incorprated in there needs to be determined using the navier stokes equation for continuity and momentum transport given as follows,

$$\nabla\cdot\vec{v} = 0 \tag{3.20}$$

$$\frac{\partial\vec{u}}{\partial t} = -\nabla P + \nu\nabla^2\left(\vec{u}^2\right) - \vec{u}\cdot\nabla\left(\vec{u}\right) \tag{3.21}$$

The equations needed to be modified to correctly simulate flow around the evolving solid phase, ensuring the no slip condition at the solid-liquid interface. We resorted to a description utilised by Steinbach [3], where in the diffuse

interface region is viewed as a rigid porous medium. Here, the usual no-slip condition at the sharp solid- liquid interface is enforced through a varying inter facial force term $(1-\phi)$ in the diffuse interface region. The mass and momentum conservation equations can then be written, respectively as,

$$\nabla \cdot [(1-\phi)\vec{v}] = 0 \tag{3.22}$$

$$\frac{\partial \vec{v}(1-\phi)}{\partial t} = -(1-\phi)\nabla P + \nu\nabla^2\left(\vec{v}(1-\phi)\right) - \vec{v}\cdot\nabla\left(\vec{v}(1-\phi)\right) \tag{3.23}$$

The above modification to the Navier Stokes equation was utilised for integrating mass transport in fluid phase into our model.

Implementation and Results

4.1 One Dimensional Solidification Profile

As a first test of the model, we tried to simulate solidification in one dimension for which the evoltuion profiles for state variables are well known. Mass transport is through diffusion only. We utilised an explicit implementation of the evolution euqations for ϕ and μ

$$\tau\epsilon\frac{\phi_i^{t+1}-\phi_i^t}{\Delta t}=\gamma\underbrace{\left(\frac{\phi_{i+1}^t-2\phi_i^t+\phi_{i-1}^t}{(\Delta t)^2}\right)}_{\text{laplacian of }\phi}-\frac{\gamma}{\epsilon}18\phi_i^t(1-\phi_i^t)(1-2\phi_i^t)+(k-1)\mu_i^t\left(\mu_i^t-\mu_{eq}\right)\left(6\phi_i^t\right)\left(1-\phi_i^t\right)$$

$$\chi\frac{\mu_i^{t+1}-\mu_i^t}{\Delta t}=M\underbrace{\left(\frac{\mu_{i+1}^t-2\mu_i^t+\mu_{i-1}^t}{(\Delta t)^2}\right)}_{\text{laplacian of }\mu}-6\left(k-1\right)\mu_i^t\phi_i^t\left(1-\phi_i^t\right)\frac{\partial\phi}{\partial t}$$

The evolving profiles of the phasefield vatiable, ϕ, concentration and diffusion potential μ are depicted in the following images.

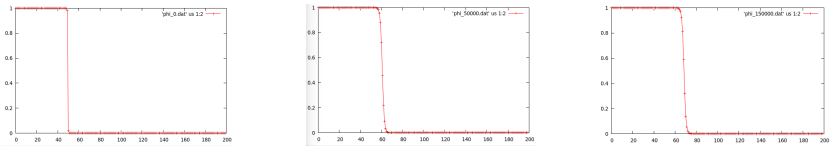

(a) timestep 0 (b) timestep 50000 (c) timestep 150000

Figure 4.1: time evolution of the phase field variable ϕ

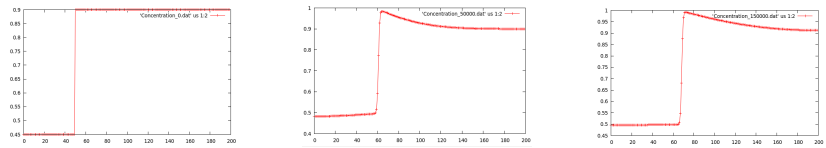

(a) timestep 0 (b) timestep 50000 (c) timestep 150000

Figure 4.2: time evolution of concentration

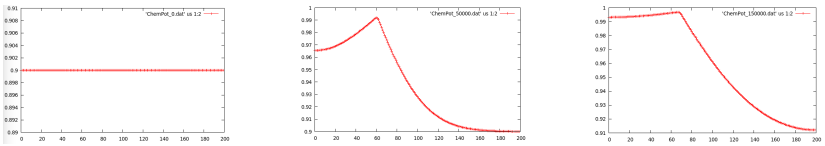

(a) timestep 0 (b) timestep 50000 (c) timestep 150000

Figure 4.3: time evolution of chemical potential μ

4.2 Isotropic Solidification in 2D - only diffusion

In two dimensions, ϕ and μ fields we represented by two 200×200 meshes. The time update is through forward difference by calcualting the partial derivatives of ϕ and μ at each node point. Also, fluid is neglected such that diffusion is the only mode transport.

$$\tau\epsilon\frac{\partial\phi}{\partial t} = \gamma\nabla^2\phi - \frac{\gamma}{\epsilon}18\phi(1-\phi)(1-2\phi) + (k-1)\mu\left(\mu-\mu_{eq}\right)(6\phi)\left(1-\phi\right)$$

$$\chi\frac{\partial\mu}{\partial t} = M\nabla^2\mu - 6\left(k-1\right)\mu\phi\left(1-\phi\right)\frac{\partial\phi}{\partial t}$$

$$\nabla^2\phi = \frac{\phi_{i+1,j}+\phi_{i-1,j}+\phi_{i,j+1}+\phi_{i,j-1}-4\phi_{i,j}}{(\Delta t)^2}$$

$$\nabla^2\mu = \frac{\mu_{i+1,j}+\mu_{i-1,j}+\mu_{i,j+1}+\mu_{i,j-1}-4\mu_{i,j}}{(\Delta t)^2}$$

Gibbs Thompson Effect

Our functional has the form of

$$\mathcal{F} = \int_{-\infty}^{\infty}(\gamma\epsilon|\nabla\phi|^2 + \frac{\gamma}{\epsilon}9\phi^2(1-\phi)^2 + ...)dx$$

By the equipartition of energy, we have for one dimension,

$$\gamma\epsilon\left(\frac{\partial\phi}{\partial x}\right)^2 = \frac{\gamma}{\epsilon}9\phi^2(1-\phi)^2$$

$$\Rightarrow \frac{\partial\phi}{\partial x} = \frac{3}{\epsilon}\phi(1-\phi)$$

Also, we know that total surface energy σ is given by the interfacing the interfacial energy term over the entire domain,

$$\sigma = \int_{-\infty}^{\infty} 2\gamma\epsilon\left(\frac{\partial\phi}{\partial x}\right)^2\cdot dx$$

$$= \int_0^1 2\gamma\epsilon\left(\frac{\partial\phi}{\partial x}\right)\cdot d\phi$$

$$= 6\gamma\int_0^1 2\phi(1-\phi)d\phi$$

$$= 6\gamma\left[\frac{\phi^2}{2} - \frac{\phi^3}{6}\right]_0^1$$

$$\Rightarrow \sigma = \gamma$$

We also know that at critical radius, surface energy equals the driving force for solidification- due to deviation of deviation from equilibrium of the Free

energy,

$$\frac{\sigma}{r} = (k-1)\mu\,(\mu - \mu_e q)$$

Thus, for a given radius we can calculate a critical μ_c for which the nuclei is stable. For $\mu > \mu_c$ nuclei should grow, otherwise the nuclei should shrink.

We used the above relation to calculate the critical μ_c for a radius of 50 units and found out that this Gibbs Thompson relation indeed holds for the present model.

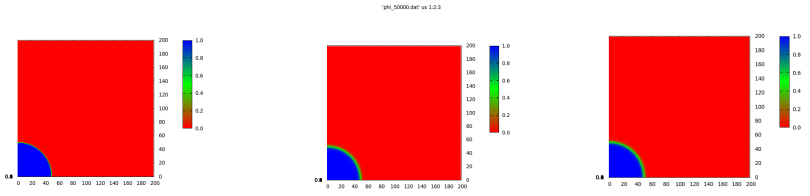

(a) timestep 0 (b) timestep 50000 (c) timestep 150000

Figure 4.4: Nuclei at critical radius - not growing

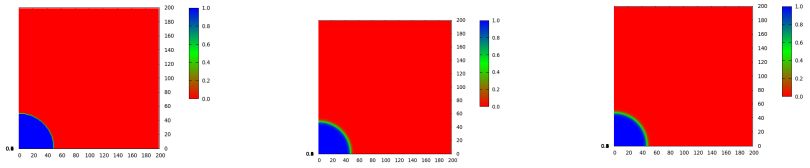

(a) timestep 0 (b) timestep 50000 (c) timestep 150000

Figure 4.5: Nuclei Shrinking - μ less than critical

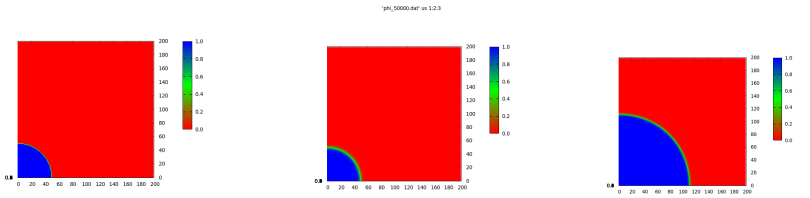

(a) timestep 0 (b) timestep 50000 (c) timestep 99000

Figure 4.6: Nuclei growing - μ greater than critical

4.3 Dendritic Solidification

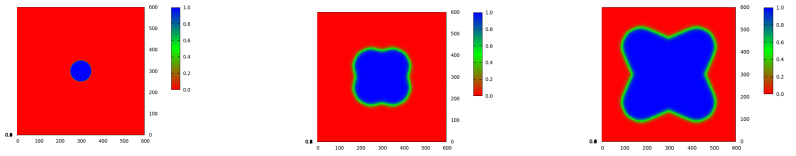

(a) timestep 0 (b) timestep 15000 (c) timestep 30000

Figure 4.7: Dendritic solidification on introducing anisotropy

4.4 Simulating fluid flow in closed space

Lid Driven Cavity Flow

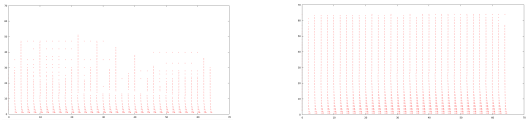

(a) timestep 0 (b) timestep 10000

Figure 4.8: Lid Driven Cavity Flow; South wall moving left

Poiseuille flow

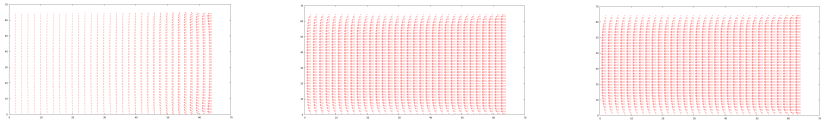

(a) timestep 1000 (b) timestep 10000 (c) timestep 50000

Figure 4.9: Pressure difference between East and West walls

Flow around a solid object in a closed space

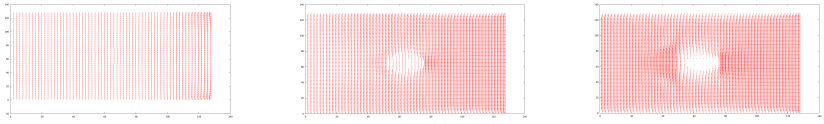

(a) timestep 1000 (b) timestep 10000 (c) timestep 50000

Figure 4.10: Flow around a solid with a diffuse interface

Discretisation

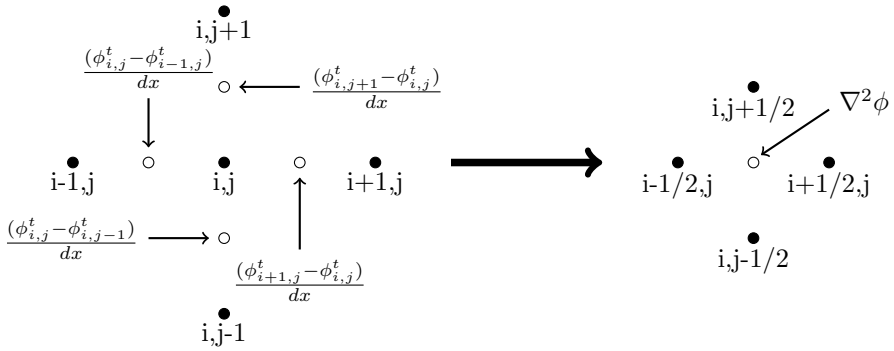

Fig 7: Discretization of the domain for calculating the Laplacian of ϕ.

Bibliography

[1] J.S. Langer, in Chance and Matter edited by J. Souletie, J. Vannenimus and R Stora (North Holland, Amsterdam 1987), p. 629; D Kessler, J Koplik and H Levine, Adv. Phys. 37, 255 (1988); E .A. Brenner and V.I. Mel'nikov, *ibid.* 40, 53 (1991)

[2] J. S. Langer, Phys. Rev. Lett., Volume 44, Number 15, 14 April 1980

[3] I. Steinbach, Acta Materialia 57 (2009) 2640 - 2645

[4] Tong et al., Phys. Rev. E, vol. 61, No. 1, January 2000

[5] Abhik Chaudhary and Britta Nestler, Phys. Rev. E 85,021602 (2012)

[6] Britta Nestler and Abhik Chaudhary, Current Opinion in solid State and Materials Science 15(2011) 93-105

[7] C. Beckermann et al., Jour. of Comp. Phys. 154, 468-496 (1999)

[8] W.J. Boettinger el al., Annu. Rev. Mater. Res. 2002. 32:163-94